

3.

Rational function approximation (RFA)

3.1. Introduction

The linear dynamic system of the bridge deck subjected to self-excited and buffeting wind forces was approximated by the following equations:

$$m\ddot{h} + c_h \dot{h} + k_h h = \rho U^2 B \left[K H_1^*(k) \frac{\dot{h}}{U} + K H_2^*(k) B \frac{\dot{a}}{U} + K^2 H_3^*(k) \alpha + K^2 H_4^{**}(k) \frac{h}{B} \right] - \frac{1}{2} \rho U^2 B [C_L \frac{2u}{U} + (C_L' + C_D) \frac{w}{U}] \quad (2.39)$$

$$I_\alpha \ddot{\alpha} + c_\alpha \dot{\alpha} + k_\alpha h = \rho U^2 B^2 \left[K A_1^*(k) \frac{\dot{h}}{U} + K A_2^*(k) B \frac{\dot{a}}{U} + K^2 A_3^*(k) \alpha \right] + K^2 A_4^{**}(k) \frac{h}{B} + \frac{1}{2} \rho U^2 B^2 [C_M \frac{2u}{U} + C_M' \frac{w}{U}] \quad (2.40)$$

In order to solve the equations (2.39) and (2.40), it is required that the air-force vector be available in the time domain. This is accomplished if the Laplace transform representation of (2.39) and (2.40) with zero initial conditions is used, yielding the following equations in matrix form:

$$\left[\mathbf{M} p^2 \frac{U^2}{B^2} + \mathbf{C} p \frac{U}{B} + \mathbf{K} \right] \mathcal{L}(\mathbf{q}) = [\mathbf{V}_f] [\mathbf{Q}] U^2 \mathcal{L}(\mathbf{q}) \quad (2.46)$$

where \mathbf{M} , \mathbf{C} , \mathbf{K} are the two by two diagonal mass, damping and stiffness matrices, respectively, and $[\mathbf{Q}(t)]$ represents the air-force vector in the time domain. All matrices belonging to (2.46) were presented in (2.47) to (2.50).

Equation (2.46) is said to represent a finite-state aero elastic system that can be converted into a linear, time-invariant, finite-state form to perform stability analysis of control system design if each term of the unsteady aerodynamic matrix $[Q(p)]$ can be represented by a ratio of polynomials in p . Generally the air forces can be determined only for pure oscillatory motion of a structure such as a lifting surface. However, since $[Q(p)]$ is analytic for a causal, stable, and linear system, it can be directly deduced from $[Q(p)]$, which is obtained from an oscillatory theory. This is realized by approximating each term of the generalized

air-force matrix $[Q(p)]$ by a rational polynomial in p and then solving for the coefficients of the polynomial, which gives the least-square-error fit with tabulated oscillatory air forces at given values of the reduced frequency. The transfer function matrix $[Q(p)]$ is then obtained by the replacement.

It is more convenient to use the non-dimensionalized reduced frequency $k = \omega b/U$ because the oscillatory aerodynamic data are generally available for certain reduced frequencies. When this is done, the Laplace variable also becomes non-dimensionalized such that $p = \frac{sb}{U} = \left(\frac{\omega b}{U}\right)i = ki$

There have been many approaches to this direct conversion process, as for example Roger [56] and Abel [1], who formulated a rational function approximation for three-dimensional, subsonic aerodynamics by using a series of poles to represent the aerodynamic lags attributable to the wake. The poles are chosen to be the same for all elements of the transfer matrix. The success of the fit is dependent on the choice of poles, which, in turn, is based on experience. This method is known as the conventional least-squares method because the parameters in the curve fit are determined by a least-squares technique.

Tiffany and Adams [89] used a non-gradient, non-linear optimizer to select the values of lag-parameters in the least-squares formulation, which gave the minimum total least-squared fit error with oscillatory data. Another approach, similar in many ways to the rational function of Roger [56] and Abel [1] is that of Dowell [12]. He used a series of decaying exponentials in the time domain, which in the Laplace domain is represented by a series of simple poles.

Eversman and Tewari [15] mention in the references of their article many important contributions that deal with the problem of representing the unsteady aerodynamics by rational functions. The interested reader may consult them for further research.

3.2. Least-squares Rational Function Approximation

The least-squares approximation uses a rational function represented by a second-order polynomial in the Laplace variable with an additional series of simple poles for each term of the generalized unsteady aerodynamic matrix $Q(s)$. The poles, which denote lag terms in the time domain, are common for all elements of $Q(s)$, thereby reducing considerably the number of augmented aerodynamic states compared to the case where all (or some) of the elements

are allowed to have different poles. This leads to the representation of the $\mathbf{Q}(s)$ matrix by the following approximation:

$$\hat{\mathbf{Q}}(s) = q \left\{ \mathbf{A}_0 + \mathbf{A}_1 s \left(\frac{b}{U} \right) + \mathbf{A}_2 s^2 + \left(\frac{U}{b} \right) \sum_{n=1}^{n_L} \frac{\mathbf{A}_{(n+2)}}{s + \left(\frac{U}{b} \right) \lambda_n} \right\} \quad (3.3)$$

In equation (3.3), $\hat{\mathbf{Q}}(s)$ denotes the approximation to $\mathbf{Q}(s)$ in equation (2.50), $s = \frac{pU}{B}$, λ_n are the n lag parameters, q is the free stream pressure, b is the bridge semi-width and n_L is the number of lag terms. In aeronautical applications the approximation function has the term s^2 representing the added aerodynamic mass and mass torsional moment of inertia. However, in problems of bridge aerodynamics this term is neglected and the approximation is restricted to terms in s .

This is the reason why the terms H_4^* and A_3^*

$$H_4^*(k) = -2\pi \left[\frac{1}{8} + \frac{G(k)}{4k} \right] \quad (2.20)$$

$$A_3^*(k) = \left[F(k) - \frac{k G(k)}{2} + \frac{k^2}{8} \right] \frac{\pi}{16k^2} \quad (2.24)$$

are simplified to

$$H_4^*(k) = -2\pi \left[\frac{G(k)}{4k} \right] \quad (2.35a)$$

$$A_3^*(k) = \left[F(k) - \frac{k G(k)}{2} \right] \frac{\pi}{16k^2} \quad (2.35b)$$

In so doing, the additional matrix \mathbf{A}_2 does not need to be considered in the approximation operations. The elements of \mathbf{A}_0 and \mathbf{A}_1 represent stiffness and damping respectively. The partial fractions $\frac{\mathbf{A}_{(n+2)}}{s + \left(\frac{U}{b} \right) \lambda_n}$ are commonly called lag terms (termos de retardo), because each term represents a transfer function in which the output “lags” behind the input and permits an approximation of the time delays inherent in unsteady aerodynamics.

The values of the lag parameters must be positive for the stability of the transfer function. The number of lag parameters taken directly influences the fit accuracy of the approximate aerodynamic transfer function with the frequency domain data because the lag terms account for the lag associated with circulation, which is presumably represented exactly only by an infinite number of lag terms. When the inverse Laplace transform is applied upon $\hat{\mathbf{Q}}(s)$, the approximate aerodynamic unit impulse response matrix results.

3.3. Karpel minimum-state RFA

The formulation suggested by Karpel [25], called minimum-state RFA, approximates $Q(p)$ to $\widehat{Q}(p)$ by the following rational equations:

$$\widehat{Q}(p) = A_0 + A_1 p + D(pI + R)^{-1}E \quad (3.4)$$

where $R = \begin{bmatrix} \lambda_1 & \cdots & 0 \\ \vdots & \ddots & \vdots \\ 0 & \cdots & \lambda_{n_L} \end{bmatrix}$ is the diagonal matrix of lag parameters λ_n , for $1 \leq n \leq n_L$ and $p = \frac{sb}{U} = \left(\frac{\omega b}{U}\right) i = ki$.

The matrices to be approximated are:

$$Q = \begin{bmatrix} 2K^2 H_4^* + 2K^2 H_1^* i & 2K^2 H_3^* + 2K^2 H_2^* i \\ 2K^2 A_4^* + 2K^2 A_1^* i & 2K^2 A_3^* + 2K^2 A_2^* i \end{bmatrix} \quad (2.51)$$

For two degrees of freedom and $n_L = 3$, the matrix equation (3.4) can be expressed with the size of its terms as:

$$\widehat{Q}(p) = A_0[2 \times 2] + A_1[2 \times 2] p + D[2 \times 3] \cdot \frac{1}{\begin{bmatrix} p+\lambda_1 & 0 & 0 \\ 0 & p+\lambda_2 & 0 \\ 0 & 0 & p+\lambda_3 \end{bmatrix}} \cdot E[3 \times 2] \quad (3.10)$$

The resulting state-space equations have the form:

$$Q = \begin{bmatrix} \ddot{q} \\ \dot{q} \\ \dot{x}_a \end{bmatrix} = \begin{bmatrix} -M^{-1} \left[C - \left(\frac{B}{U}\right) V_f A_1 \right] & -M^{-1} [K - V_f A_0] & M^{-1} V_f D \\ I & 0 & 0 \\ 0 & \left(\frac{U}{B}\right) E & -\left(\frac{U}{B}\right) R \end{bmatrix} \cdot \begin{bmatrix} \dot{q} \\ q \\ x_a \end{bmatrix} \quad (3.11)$$

Improvement of the approximation can be achieved by increasing the number of lag terms. However, it adversely increases the number of equations required to define the aerodynamic system. Minimization of approximation errors can also be obtained by imposing constraints on the elements of the transfer functions to match the oscillatory data at some values of the reduced frequency, but this degrades the fit at other frequencies. Thus, no constraints were imposed on the transfer function in the present thesis.

The augmented state vector contains new terms known as aerodynamic states, represented by vector x_a . In this RFA formulation, the addition of one lag term results in the addition of only one new aerodynamic state. The additional improvements may be gained by an optimization of the lag parameters. In the minimum state formulation (3.10), the numerator coefficients for the lag terms are the product elements of D and E , so the two-step iterative linear optimization is employed. First, for the selected initial R and D , the matrices A_0 , A_1 and E are

obtained through the least-squares optimization such that the total approximation error

$$\sqrt{\sum_{i=1}^2 \sum_{j=1}^2 w_{ij} e_{ij}} \quad (3.12)$$

is minimized. The weighing factor is denoted by w_{ij} , and the measure of error between the approximating curve and the actual tabular data is:

$$\varepsilon_{ij} = \frac{\sum_1^4 \|\hat{Q}_{ij}(p) - Q_{ij}(p)\|^2}{M_{ij}} \quad (3.13)$$

where

$$M_{ij} = \frac{\max}{n} \{1, \|Q_{ij}(iK_n)\|^2\} \quad (3.14)$$

In the next step, for the same \mathbf{R} and previously determined \mathbf{E} the matrices \mathbf{A}_0 , \mathbf{A}_1 and new \mathbf{E} are computed. These steps are repeated till the global approximation error (3.13) converges or reaches the stopping criterion of a maximum number of iterations.

The lag parameters λ_i are in the denominator and are found via the nonlinear no-gradient optimizer proposed by Nelder & Mead [47]. The range of variation is the range of reduced frequencies in the available tabular data, i.e.

$$0 \leq L_1 \leq \lambda_i \leq U_1 \quad (3.15)$$

These side constraints are enforced by an inverse sinusoidal transformation of the design space $[L_1, U_1]$ onto the real line segment $[-1, 1]$. The relationship between them is:

$$\lambda_i = \frac{U_1 - L_1}{2} \sin\left(\frac{\pi}{2} z_1\right) + \frac{U_1 + L_1}{2} \quad (3.16)$$

$$-1 \leq z_1 \leq 1 \quad (3.17)$$

This transformation ensures that the side constraints are always satisfied. A Fortran program written by Masukawa [43], to model unsteady aerodynamic forces of various bridge decks is used throughout this work. Besides checking the modeling matrices \mathbf{A}_0 , \mathbf{A}_1 , \mathbf{C} , \mathbf{D} , \mathbf{R} reported by Wilde [96] for the case of the flat plate, the aerodynamic derivatives of eight different bridge profiles, reported by Starossek [81] will be also modeled, using Masukawa's program, which in fact follows the procedure stated by Nelder and Mead [47].

3.4. Numerical examples

The time domain modeling of unsteady aerodynamics of a bridge deck, described in the previous chapter, can be applied to any experimentally determined flutter derivatives. This was the objective of Masukawa's Master thesis [43] (in Japanese). Results of rational function approximations of flat and bluff decks and trusses and rectangular girder cross section are partially presented by Scanlan et al. [66] and [67], by Wilde et al. [95] and [99], as well as in Masukawa's Master thesis [43], a copy of which was obtained by the library of the Pontifícia Universidade Católica do Rio de Janeiro.

The program was applied to the modeling of the aerodynamic derivatives of eight different profiles reported by Starossek [81]. The same procedure can be repeated by bridge designers to other cross sections, provided the derivatives of the profile under investigation are known, as well as the corresponding dynamic data.

The example to be discussed in items 3.4.1 and 3.4.2 is the general case where the flutter derivatives are computed by the theoretical formulation of Theodorsen [84], adapted by Scanlan and Tomko [66], and revised later by Simiu and Scanlan [67] expresses Scanlan derivatives by the following formulae, repeated below for reasons of convenience:

$$H_1^*(k) = 2\pi F(k)/4k ; \quad A_1^*(k) = \pi F(k)/8k \quad (2.17), (2.22)$$

$$H_2^*(k) = (\pi/8k) [1 + 2G(k)/k + F(k)] \quad (2.18)$$

$$H_3^*(k) = (2\pi/8k^2)[F(k) - k G(k)/2] \quad (2.19)$$

$$H_4^{**}(k) = (-\pi/4)(2G(k)/k); \quad A_4^*(k) = -\pi G(k)/8k \quad (2.36a), (2.22)$$

$$A_2^*(k) = (\pi/32k) [F(k) - 1 + 2G(k)/k] \quad (2.23)$$

$$A_3^{**}(k) = (\pi/16k^2)[F(k) - kG(k)/2] \quad (2.36b)$$

Next, these terms are rearranged to produce the **Q** matrix:

$$Q = \begin{bmatrix} 2K^2 H_4^* + p \ 2KH_1^* & 2K^2 H_3^* + p \ 2KH_2^* \\ 2K^2 A_4^* + p \ 2KA_1^* & 2K^2 A_3^* + p \ 2KA_2^* \end{bmatrix} \quad (3.18)$$

Matrix $\hat{Q}(p)$, i.e., the approximation of matrix **Q**, reads:

$$\hat{Q}(p) = \mathbf{A}_0[2 \times 2] + \mathbf{A}_1[2 \times 2]p + \mathbf{D}[2 \times n_L] \begin{bmatrix} 1 & & & \\ p+\lambda_1 & \cdots & & 0 \\ \vdots & \ddots & \ddots & \vdots \\ 0 & \cdots & & p+\lambda_{n_L} \end{bmatrix} \mathbf{E}[n_L \times 2]$$

where n_L is the number of lag terms and \mathbf{A}_0 , \mathbf{A}_1 , \mathbf{D} , $(\mathbf{pI} + \mathbf{R})$, \mathbf{E} are obtained by Karpel's minimum state RFA method. Considering two lag terms λ_1, λ_2 only, the full expressions of \hat{Q}_{11} , \hat{Q}_{12} , \hat{Q}_{21} , \hat{Q}_{22} read:

$$\hat{Q}_{11} = \begin{bmatrix} a_{011} + a_{111} \cdot K_1 \cdot i + \frac{d_{11} \cdot e_{11}}{\lambda_1 + K_1 \cdot i} + \frac{d_{12} \cdot e_{21}}{\lambda_2 + K_1 \cdot i} \\ a_{011} + a_{111} \cdot K_2 \cdot i + \frac{d_{11} \cdot e_{11}}{\lambda_1 + K_2 \cdot i} + \frac{d_{12} \cdot e_{21}}{\lambda_2 + K_2 \cdot i} \\ a_{011} + a_{111} \cdot K_3 \cdot i + \frac{d_{11} \cdot e_{11}}{\lambda_1 + K_3 \cdot i} + \frac{d_{12} \cdot e_{21}}{\lambda_2 + K_3 \cdot i} \\ a_{011} + a_{111} \cdot K_4 \cdot i + \frac{d_{11} \cdot e_{11}}{\lambda_1 + K_4 \cdot i} + \frac{d_{12} \cdot e_{21}}{\lambda_2 + K_4 \cdot i} \\ a_{011} + a_{111} \cdot K_5 \cdot i + \frac{d_{11} \cdot e_{11}}{\lambda_1 + K_5 \cdot i} + \frac{d_{12} \cdot e_{21}}{\lambda_2 + K_5 \cdot i} \\ a_{011} + a_{111} \cdot K_6 \cdot i + \frac{d_{11} \cdot e_{11}}{\lambda_1 + K_6 \cdot i} + \frac{d_{12} \cdot e_{21}}{\lambda_2 + K_6 \cdot i} \\ a_{011} + a_{111} \cdot K_7 \cdot i + \frac{d_{11} \cdot e_{11}}{\lambda_1 + K_7 \cdot i} + \frac{d_{12} \cdot e_{21}}{\lambda_2 + K_7 \cdot i} \\ a_{011} + a_{111} \cdot K_8 \cdot i + \frac{d_{11} \cdot e_{11}}{\lambda_1 + K_8 \cdot i} + \frac{d_{12} \cdot e_{21}}{\lambda_2 + K_8 \cdot i} \\ a_{011} + a_{111} \cdot K_9 \cdot i + \frac{d_{11} \cdot e_{11}}{\lambda_1 + K_9 \cdot i} + \frac{d_{12} \cdot e_{21}}{\lambda_2 + K_9 \cdot i} \\ a_{011} + a_{111} \cdot K_{10} \cdot i + \frac{d_{11} \cdot e_{11}}{\lambda_1 + K_{10} \cdot i} + \frac{d_{12} \cdot e_{21}}{\lambda_2 + K_{10} \cdot i} \end{bmatrix} \quad (3.19a)$$

$$\hat{Q}_{12} = \begin{bmatrix} a_{012} + a_{112} \cdot K_1 \cdot i + \frac{d_{11} \cdot e_{12}}{\lambda_1 + K_1 \cdot i} + \frac{d_{12} \cdot e_{22}}{\lambda_2 + K_1 \cdot i} \\ a_{012} + a_{112} \cdot K_2 \cdot i + \frac{d_{11} \cdot e_{12}}{\lambda_1 + K_2 \cdot i} + \frac{d_{12} \cdot e_{22}}{\lambda_2 + K_2 \cdot i} \\ a_{012} + a_{112} \cdot K_3 \cdot i + \frac{d_{11} \cdot e_{12}}{\lambda_1 + K_3 \cdot i} + \frac{d_{12} \cdot e_{22}}{\lambda_2 + K_3 \cdot i} \\ a_{012} + a_{112} \cdot K_4 \cdot i + \frac{d_{11} \cdot e_{12}}{\lambda_1 + K_4 \cdot i} + \frac{d_{12} \cdot e_{22}}{\lambda_2 + K_4 \cdot i} \\ a_{012} + a_{112} \cdot K_5 \cdot i + \frac{d_{11} \cdot e_{12}}{\lambda_1 + K_5 \cdot i} + \frac{d_{12} \cdot e_{22}}{\lambda_2 + K_5 \cdot i} \\ a_{012} + a_{112} \cdot K_6 \cdot i + \frac{d_{11} \cdot e_{12}}{\lambda_1 + K_6 \cdot i} + \frac{d_{12} \cdot e_{22}}{\lambda_2 + K_6 \cdot i} \\ a_{012} + a_{112} \cdot K_7 \cdot i + \frac{d_{11} \cdot e_{12}}{\lambda_1 + K_7 \cdot i} + \frac{d_{12} \cdot e_{22}}{\lambda_2 + K_7 \cdot i} \\ a_{012} + a_{112} \cdot K_8 \cdot i + \frac{d_{11} \cdot e_{12}}{\lambda_1 + K_8 \cdot i} + \frac{d_{12} \cdot e_{22}}{\lambda_2 + K_8 \cdot i} \\ a_{012} + a_{112} \cdot K_9 \cdot i + \frac{d_{11} \cdot e_{12}}{\lambda_1 + K_9 \cdot i} + \frac{d_{12} \cdot e_{22}}{\lambda_2 + K_9 \cdot i} \\ a_{012} + a_{112} \cdot K_{10} \cdot i + \frac{d_{11} \cdot e_{12}}{\lambda_1 + K_{10} \cdot i} + \frac{d_{12} \cdot e_{22}}{\lambda_2 + K_{10} \cdot i} \end{bmatrix} \quad (3.19b)$$

Figure 3-1 - Full expressions of \hat{Q}_{11} , \hat{Q}_{12} , as approximations of Q_{11} , Q_{12} .

$$\hat{Q}_{21} = \begin{bmatrix} a_{021} + a_{121} \cdot K_1 \cdot i + \frac{d_{21} \cdot e_{11}}{\lambda_1 + K_1 \cdot i} + \frac{d_{22} \cdot e_{21}}{\lambda_2 + K_1 \cdot i} \\ a_{021} + a_{121} \cdot K_2 \cdot i + \frac{d_{21} \cdot e_{11}}{\lambda_1 + K_2 \cdot i} + \frac{d_{22} \cdot e_{21}}{\lambda_2 + K_2 \cdot i} \\ a_{021} + a_{121} \cdot K_3 \cdot i + \frac{d_{21} \cdot e_{11}}{\lambda_1 + K_3 \cdot i} + \frac{d_{22} \cdot e_{21}}{\lambda_2 + K_3 \cdot i} \\ a_{021} + a_{121} \cdot K_4 \cdot i + \frac{d_{21} \cdot e_{11}}{\lambda_1 + K_4 \cdot i} + \frac{d_{22} \cdot e_{21}}{\lambda_2 + K_4 \cdot i} \\ a_{021} + a_{121} \cdot K_5 \cdot i + \frac{d_{21} \cdot e_{11}}{\lambda_1 + K_5 \cdot i} + \frac{d_{22} \cdot e_{21}}{\lambda_2 + K_5 \cdot i} \\ a_{021} + a_{121} \cdot K_6 \cdot i + \frac{d_{21} \cdot e_{11}}{\lambda_1 + K_6 \cdot i} + \frac{d_{22} \cdot e_{21}}{\lambda_2 + K_6 \cdot i} \\ a_{021} + a_{121} \cdot K_7 \cdot i + \frac{d_{21} \cdot e_{11}}{\lambda_1 + K_7 \cdot i} + \frac{d_{22} \cdot e_{21}}{\lambda_2 + K_7 \cdot i} \\ a_{021} + a_{121} \cdot K_8 \cdot i + \frac{d_{21} \cdot e_{11}}{\lambda_1 + K_8 \cdot i} + \frac{d_{22} \cdot e_{21}}{\lambda_2 + K_8 \cdot i} \\ a_{021} + a_{121} \cdot K_9 \cdot i + \frac{d_{21} \cdot e_{11}}{\lambda_1 + K_9 \cdot i} + \frac{d_{22} \cdot e_{21}}{\lambda_2 + K_9 \cdot i} \\ a_{021} + a_{121} \cdot K_{10} \cdot i + \frac{d_{21} \cdot e_{11}}{\lambda_1 + K_{10} \cdot i} + \frac{d_{22} \cdot e_{21}}{\lambda_2 + K_{10} \cdot i} \end{bmatrix} \quad (3.20a)$$

$$\hat{Q}_{22} = \begin{bmatrix} a_{022} + a_{122} \cdot K_1 \cdot i + \frac{d_{21} \cdot e_{12}}{\lambda_1 + K_2 \cdot i} + \frac{d_{22} \cdot e_{22}}{\lambda_2 + K_2 \cdot i} \\ a_{022} + a_{122} \cdot K_1 \cdot i + \frac{d_{21} \cdot e_{12}}{\lambda_1 + K_2 \cdot i} + \frac{d_{22} \cdot e_{22}}{\lambda_2 + K_2 \cdot i} \\ a_{022} + a_{122} \cdot K_1 \cdot i + \frac{d_{21} \cdot e_{12}}{\lambda_1 + K_2 \cdot i} + \frac{d_{22} \cdot e_{22}}{\lambda_2 + K_2 \cdot i} \\ a_{022} + a_{122} \cdot K_1 \cdot i + \frac{d_{21} \cdot e_{12}}{\lambda_1 + K_2 \cdot i} + \frac{d_{22} \cdot e_{22}}{\lambda_2 + K_2 \cdot i} \\ a_{022} + a_{122} \cdot K_1 \cdot i + \frac{d_{21} \cdot e_{12}}{\lambda_1 + K_2 \cdot i} + \frac{d_{22} \cdot e_{22}}{\lambda_2 + K_2 \cdot i} \\ a_{022} + a_{122} \cdot K_1 \cdot i + \frac{d_{21} \cdot e_{12}}{\lambda_1 + K_2 \cdot i} + \frac{d_{22} \cdot e_{22}}{\lambda_2 + K_2 \cdot i} \\ a_{022} + a_{122} \cdot K_1 \cdot i + \frac{d_{21} \cdot e_{12}}{\lambda_1 + K_2 \cdot i} + \frac{d_{22} \cdot e_{22}}{\lambda_2 + K_2 \cdot i} \\ a_{022} + a_{122} \cdot K_1 \cdot i + \frac{d_{21} \cdot e_{12}}{\lambda_1 + K_2 \cdot i} + \frac{d_{22} \cdot e_{22}}{\lambda_2 + K_2 \cdot i} \\ a_{022} + a_{122} \cdot K_1 \cdot i + \frac{d_{21} \cdot e_{12}}{\lambda_1 + K_2 \cdot i} + \frac{d_{22} \cdot e_{22}}{\lambda_2 + K_2 \cdot i} \\ a_{022} + a_{122} \cdot K_1 \cdot i + \frac{d_{21} \cdot e_{12}}{\lambda_1 + K_2 \cdot i} + \frac{d_{22} \cdot e_{22}}{\lambda_2 + K_2 \cdot i} \end{bmatrix} \quad (3.20b)$$

Figure 3-2 - Full expressions of \hat{Q}_{21} , \hat{Q}_{22} , as approximations of Q_{21} , Q_2 .

3.4.1 The flat plate case, $0.1 \leq K \leq 1.0$ or $0.05 \leq k \leq 0.5$

Table 2-5 in Chapter 2 shows the variables Q_{ij} for the bridge deck as a flat plate, corresponding to the reduced frequencies $0.1 \leq K \leq 1.0$.

Wilde [95] specifies the following matrices for the approximation of Q_{ij} by rational functions (valid for $0.1 < K < 1.0$):

$$A_0 = \begin{bmatrix} 1.3043 & 3.5334 \\ 0.3354 & 0.8738 \end{bmatrix} \quad (3.21)$$

$$A_1 = \begin{bmatrix} 3.3842 & 2.3576 \\ 0.7989 & -0.1875 \end{bmatrix} \quad (3.22)$$

$$D = \begin{bmatrix} 3.4691 & 3.2670 \\ 0.8526 & 0.8641 \end{bmatrix}; E = \begin{bmatrix} -0.0145 & 0.0782 \\ -0.2304 & 0.2595 \end{bmatrix} \quad (3.23)$$

$$\lambda_1 = 0.1912; \lambda_2 = 0.7477 \quad (3.24)$$

A MATLAB program was written to plot the tabular data corresponding to the table “derivatives x reduced frequencies” and the approximation values using the rational functions given by equations (3.20) and matrices (3.21) to (3.24). These plots are shown in Figure 3-3 .

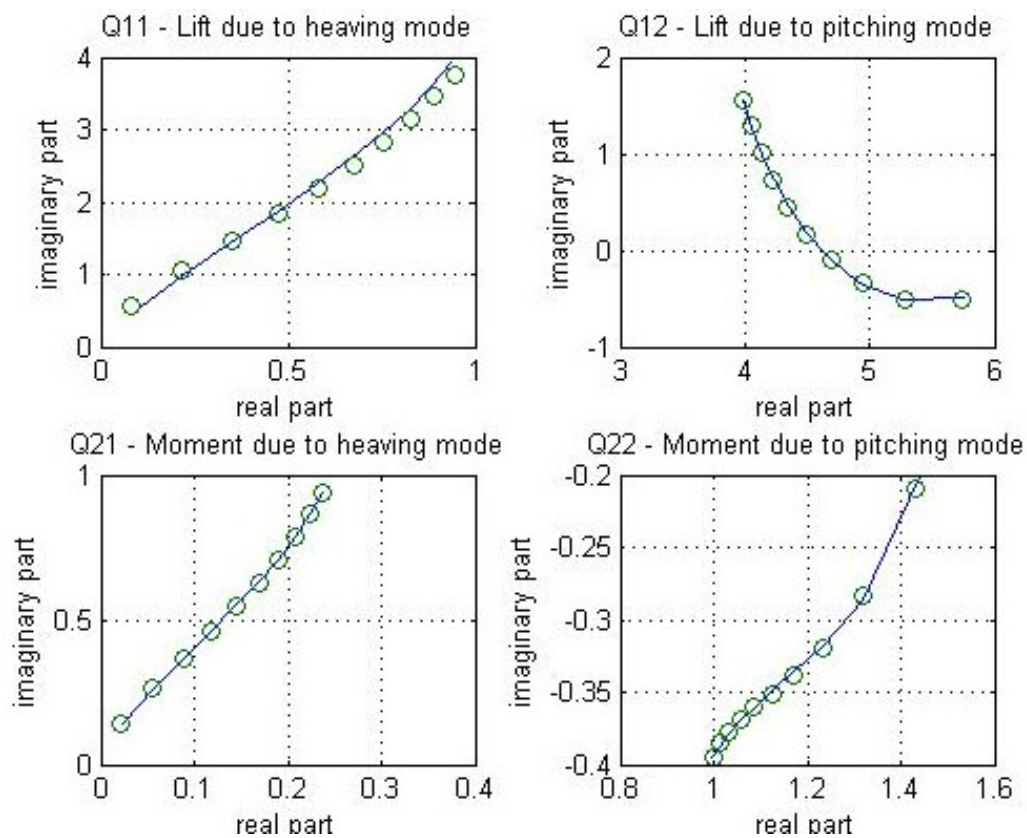


Figure 3-3 - Plots of exact and approximate values of $Q(p)$ for a flat plate using Wilde's results, valid for $0.1 < K < 1.0$ and 2 lag terms.

3.4.2 The winglets

The FORTRAN program was used to calculate the approximating functions

$$\hat{Q}(p) = A_0[2 \times 2] + A_1[2 \times 2]p + D[2 \times n_L] \begin{bmatrix} 1 \\ p+\lambda_1 & \dots & 0 \\ \vdots & \ddots & \vdots \\ 0 & \dots & p+\lambda_{n_L} \end{bmatrix} E[n_L \times 2]$$

for the winglets (reduced frequencies $0.01 \leq K \leq 0.1$ or $0.005 \leq k \leq 0.05$). The errors J and ε_{ij} were also calculated by this program. The variables Q_{ij} for the case of the winglets, i.e., for Q_{ij} corresponding to the reduced frequencies $0.01 \leq K \leq 0.1$ or $0.005 \leq k \leq 0.05$, are calculated in sequence by three EXCEL spreadsheets, shown in Table 3-1, Table 3-2 and Table 3-3. Notice that the reduced frequencies are one tenth of the reduced frequencies corresponding to the flat plate, equal to the width ratio of the winglets to the bridge deck. The matrices are shown below, for 2 lag terms

$$A_0 = \begin{bmatrix} 0.3834 & 4.4804 \\ 0.0958 & 1.1201 \end{bmatrix}; \quad A_1 = \begin{bmatrix} 4.1688 & 1.6483 \\ 1.0422 & -0.3736 \end{bmatrix}$$

$$D = \begin{bmatrix} 6.7566 & 2.1447 \\ 1.6882 & 0.5362 \end{bmatrix}; \quad E = \begin{bmatrix} -0.2845e-04 & 0.1197e-02 \\ -0.03492 & 0.1423 \end{bmatrix}$$

$$\lambda_1 = 0.03374564; \lambda_2 = 0.1986877$$

K	k	J0	J1	Y0	Y1	F	G
0.0000	0.0000	1.0000	0.0000	-7.4032	-63661.9772	1.0000	-0.0001
0.0100	0.0050	1.0000	0.0025	-3.4468	-127.3334	0.9915	-0.0266
0.0200	0.0100	1.0000	0.0050	-3.0055	-63.6786	0.9824	-0.0457
0.0300	0.0150	0.9999	0.0075	-2.7472	-42.4643	0.9731	-0.0615
0.0400	0.0200	0.9999	0.0100	-2.5640	-31.8598	0.9637	-0.0752
0.0500	0.0250	0.9998	0.0125	-2.4217	-25.4990	0.9543	-0.0872
0.0600	0.0300	0.9998	0.0150	-2.3055	-21.2600	0.9450	-0.0979
0.0700	0.0350	0.9997	0.0175	-2.2071	-18.2333	0.9358	-0.1074
0.0800	0.0400	0.9996	0.0200	-2.1219	-15.9643	0.9267	-0.1160
0.0900	0.0450	0.9995	0.0225	-2.0467	-14.2003	0.9178	-0.1237
0.1000	0.0500	0.9994	0.0250	-1.9793	-12.7899	0.9090	-0.1306

Table 3-1 - Auxiliary variables for the calculation of the derivatives of a flat plate, valid for $0 \leq k \leq 0.05$, $0 \leq K \leq 0.10$.

The overall square root error is:

$$J = \sum_{j=1}^{n=4} \sum_{i=1}^{n=4} w_{ij} \varepsilon_{ij} = 0.3752877E-02.$$

The errors of each one of the four approximations for $n = 10$ are:

$$\varepsilon_{ij} = \sum_1^n [\hat{Q}_{ij}(p) - Q_{ij}(p)]^2 / M_{ij}$$

$$\varepsilon_{ij} = [0.3245 E - 05 \quad 0.5276 E - 05 \quad 0.2033E - 06 \quad 0.5359E - 05]$$

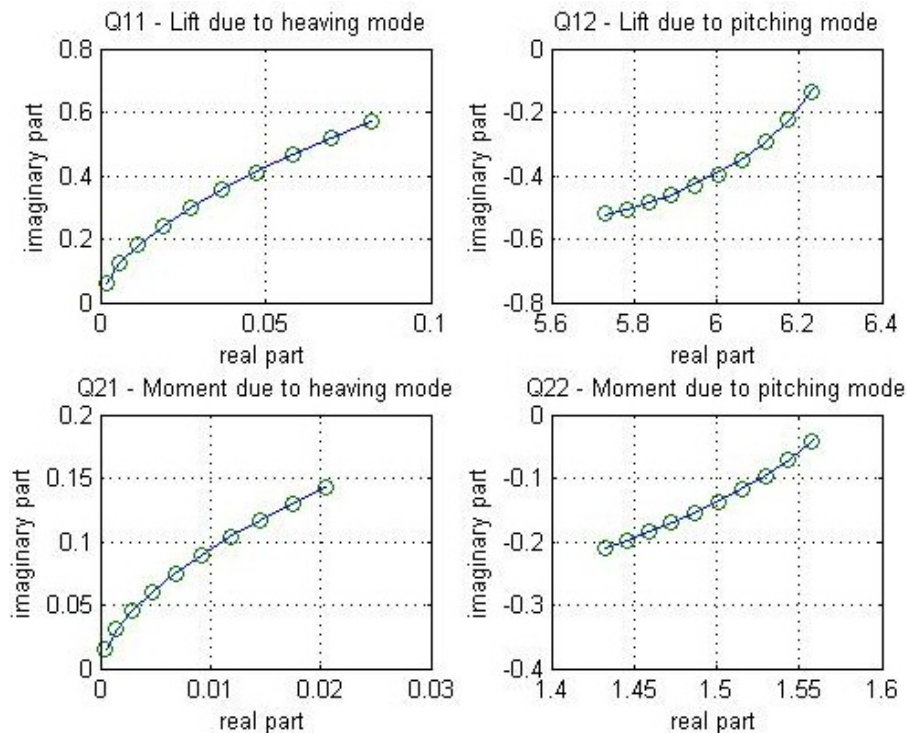
K	k	$H_{i,i=1,4}^*$ to $A_{i,i=1,4}^*$, $i=1,4$ according to (2.17) to (2.25)							
		H_1^*	H_2^*	H_3^*	H_4^*	A_1^*	A_2^*	A_3^*	A_4^*
0.00	0.000	157077.16	-834760.39	7.8539E+09	18.2660	3.9269E+04	-2.2833E+05	1.9635E+09	4.57
0.01	0.005	311.49	-680.19	31150.77	8.3660	77.8717	-209.3170	7787.69	2.09
0.02	0.010	154.32	-280.70	7717.71	7.1710	38.5796	-89.8103	1929.43	1.79
0.03	0.015	101.90	-163.06	3398.43	6.4415	25.4761	-53.8554	849.61	1.61
0.04	0.020	75.69	-109.11	1893.75	5.9068	18.9227	-37.0957	473.44	1.48
0.05	0.025	59.96	-78.93	1200.63	5.4814	14.9907	-27.5861	300.16	1.37
0.06	0.030	49.48	-59.99	825.96	5.1267	12.3702	-21.5414	206.49	1.28
0.07	0.035	42.00	-47.17	601.18	4.8222	10.4995	-17.4024	150.29	1.21
0.08	0.040	36.39	-38.03	456.03	4.5554	9.0979	-14.4154	114.01	1.14
0.09	0.045	32.04	-31.24	357.04	4.3179	8.0091	-12.1737	89.26	1.08
0.10	0.050	28.56	-26.05	286.60	4.1043	7.1393	-10.4394	71.65	1.03

Table 3-2 - Derivatives of a flat plate, valid for $0 \leq k \leq 0.05$, $0 \leq K \leq 0.10$.

K	k	Q_{11r} $=2*K^2*H_4^{**}$	Q_{11i} $=2*K^2*H_1^{**}$	Q_{12r} $=2*K^2*H_3^{**}$	Q_{12i} $=2*K^2*H_2^{**}$	Q_{21r} $=2*K^2*A_4^{**}$	Q_{21i} $=2*K^2*A_1^{**}$	Q_{22r} $=2*K^2*A_3^{**}$	Q_{22i} $=2*K^2*A_2^{**}$
0.01	0.005	0.0017	0.0623	6.2302	-0.1360	0.0004	0.0156	1.5575	-0.0419
0.02	0.01	0.0057	0.1235	6.1742	-0.2246	0.0014	0.0309	1.5435	-0.0718
0.03	0.015	0.0116	0.1834	6.1172	-0.2935	0.0029	0.0459	1.5293	-0.0969
0.04	0.02	0.0189	0.2422	6.0600	-0.3492	0.0047	0.0606	1.5150	-0.1187
0.05	0.025	0.0274	0.2998	6.0031	-0.3946	0.0069	0.0750	1.5008	-0.1379
0.06	0.03	0.0369	0.3563	5.9469	-0.4319	0.0092	0.0891	1.4867	-0.1551
0.07	0.035	0.0473	0.4116	5.8916	-0.4623	0.0118	0.1029	1.4729	-0.1705
0.08	0.04	0.0583	0.4658	5.8372	-0.4867	0.0146	0.1165	1.4593	-0.1845
0.09	0.045	0.0700	0.5190	5.7840	-0.5061	0.0175	0.1297	1.4460	-0.1972
0.1	0.05	0.0821	0.5711	5.7320	-0.5210	0.0205	0.1428	1.4330	-0.2088

Table 3-3 – Terms Q_{ij} for the winglets, valid for $0.005 \leq k \leq 0.05$, $0.01 \leq K \leq 0.10$, to be approximated by rational functions

Plots and are presented in Figure 3-4.

Figure 3-4 - Plots of exact and approximate values of $Q(p)$ corresponding to the reduced frequencies $0.01 < K < 0.10$ (winglets case).

3.4.3 Eight typical bridge profiles

The same FORTRAN program was used to calculate the approximating functions:

$$\hat{\mathbf{Q}}(p) = \mathbf{A}_0[2 \times 2] + \mathbf{A}_1[2 \times 2]p + \mathbf{D}[2 \times n_L] \begin{bmatrix} 1 \\ p+\lambda_1 & \dots & 0 \\ \vdots & \ddots & \vdots \\ 0 & \dots & p+\lambda_{n_L} \end{bmatrix} \mathbf{E}[n_L \times 2]$$

for the aerodynamic derivatives of the profiles shown in Figure 3-5, reported by Starossek [81] and Starossek et al. [75]. The complete results are shown in item D of the Appendix C. Plots of the unsteady derivatives are shown in item 3.5.

It is worth noting that, if the unsteady derivatives behave like those of a flat plate, the approximating curves are close to the experimental data. If not, as for example the Tacoma profile, the approximating curves functions, represented by matrices $\mathbf{A}_0, \mathbf{A}_1, \mathbf{D}, \mathbf{E}, \mathbf{R}$, do not match well the experimental data.

This may be explained by the fact that the Tacoma profile does not behave like aerodynamic profiles and therefore the Theodorsen functions do not represent their physical behavior when subjected to the fluid pressure.

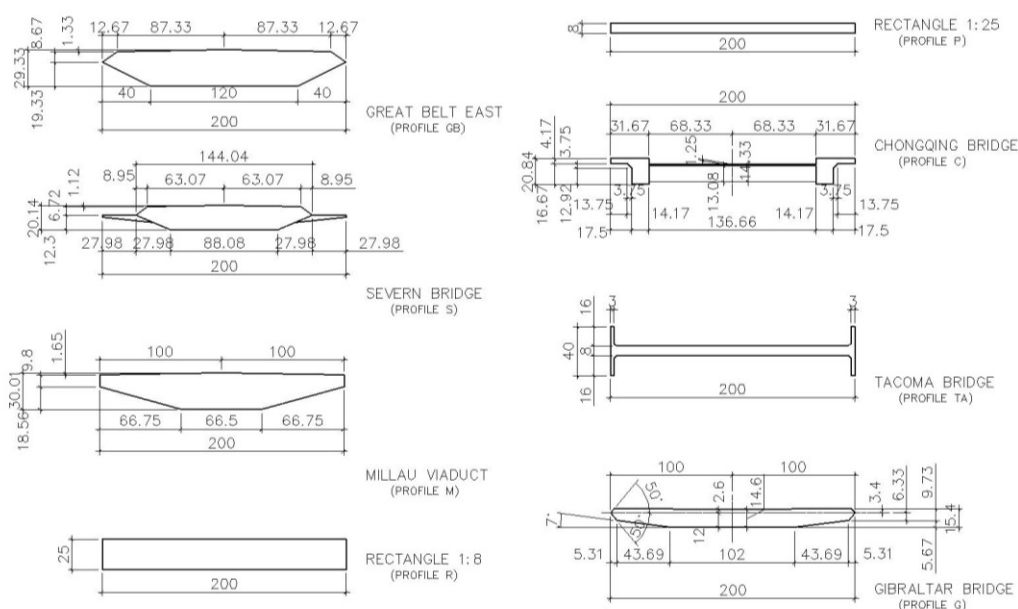


Figure 3-5- Investigated profiles of typical bridge decks.

3.5. Plots of the unsteady aerodynamic data for eight bridge profiles

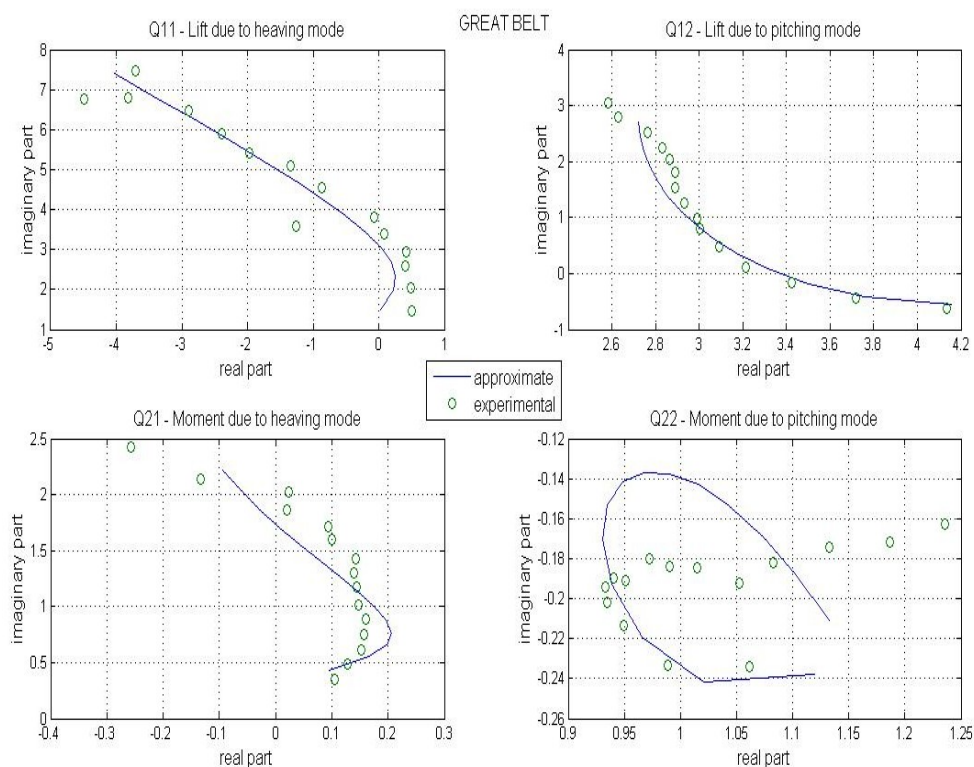


Figure 3-6 - Plots of GB unsteady aerodynamic data

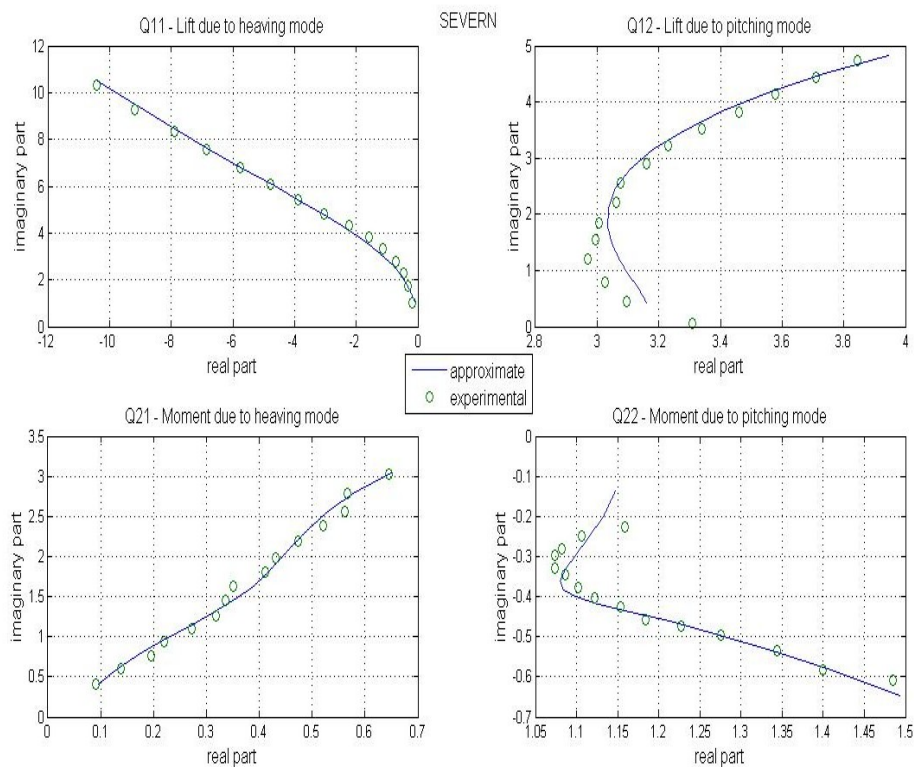


Figure 3-7 - Plots of S unsteady aerodynamic data

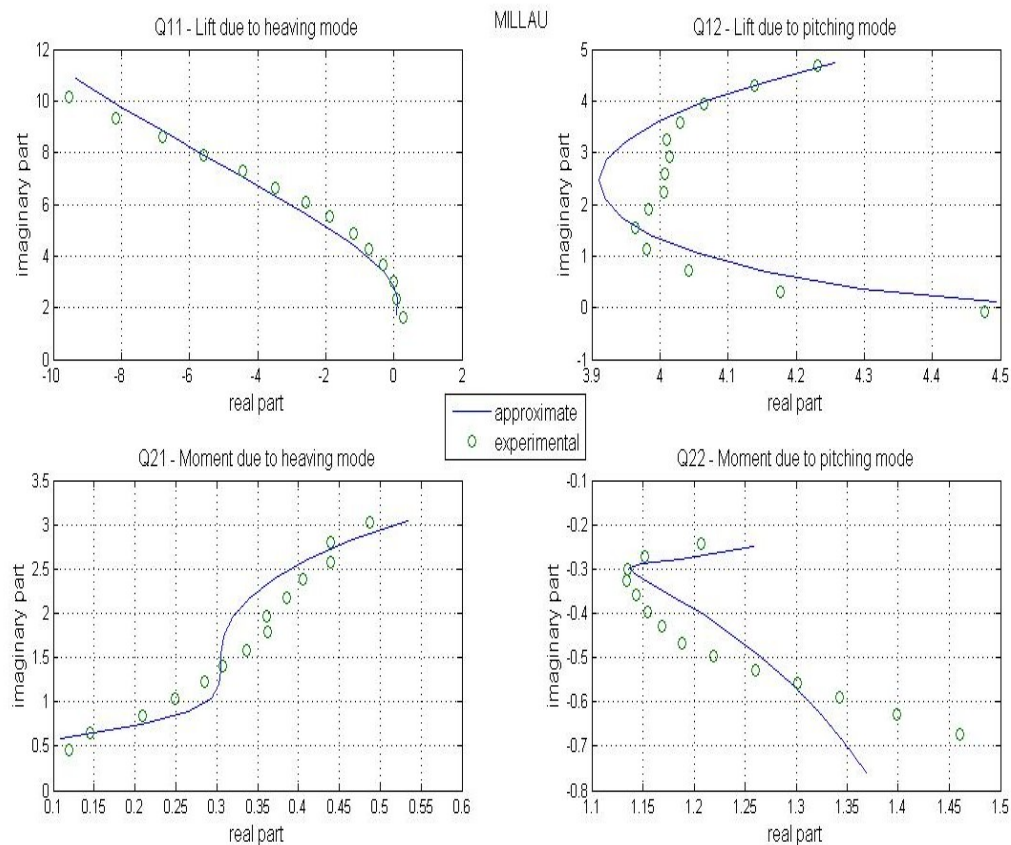


Figure 3-8 - Plots of M unsteady aerodynamic data

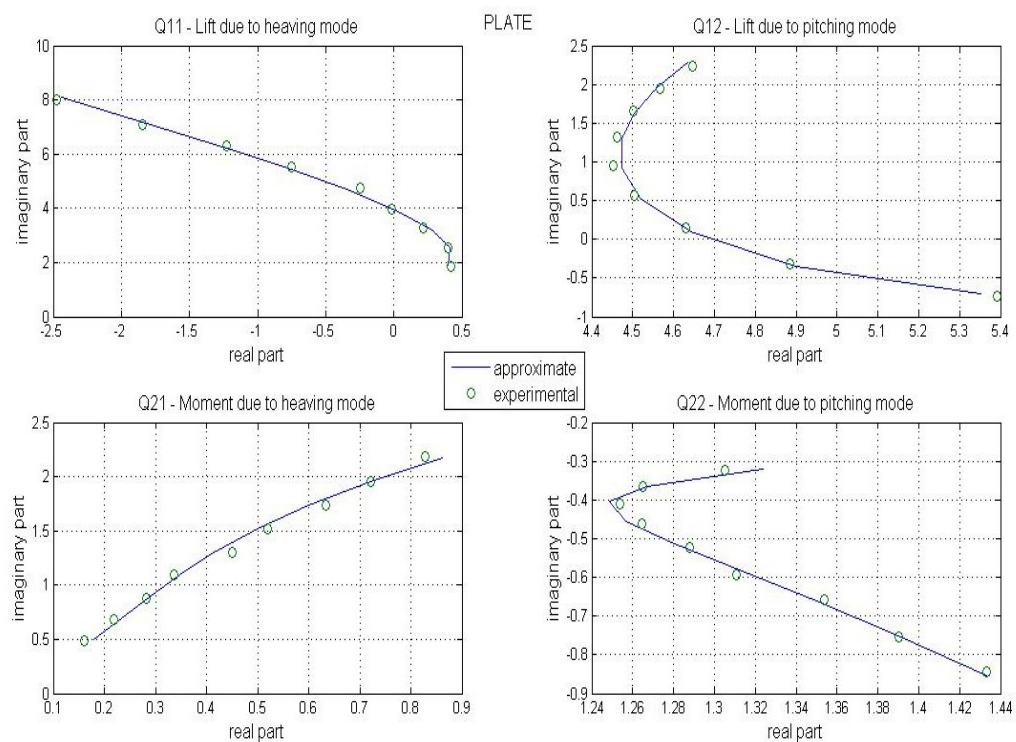


Figure 3-9 - Plots of P unsteady aerodynamic data

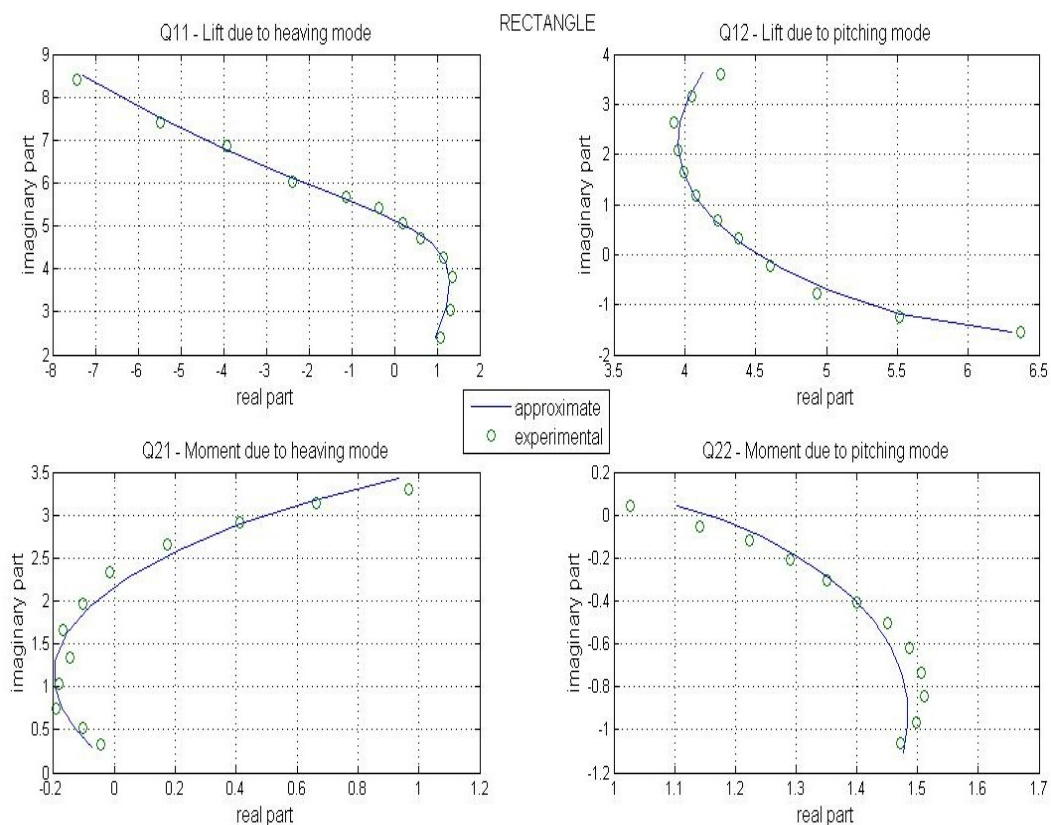


Figure 3-10 - Plots of R unsteady aerodynamic data

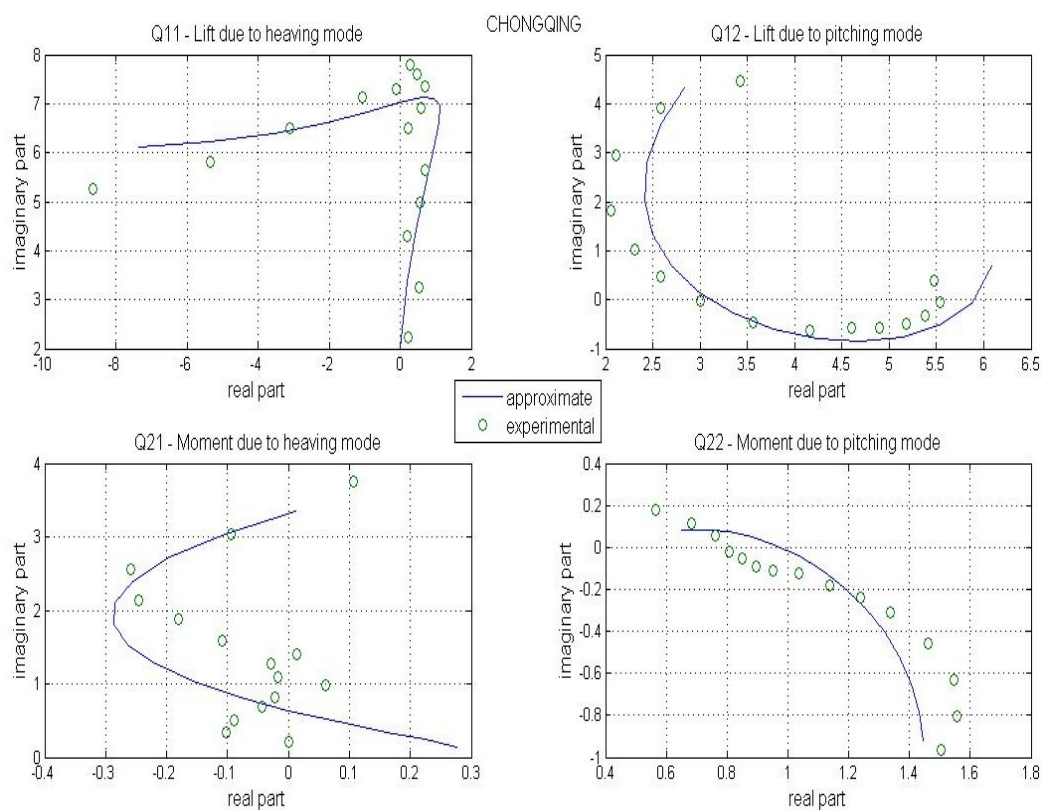


Figure 3-11 - Plots of C unsteady aerodynamic data

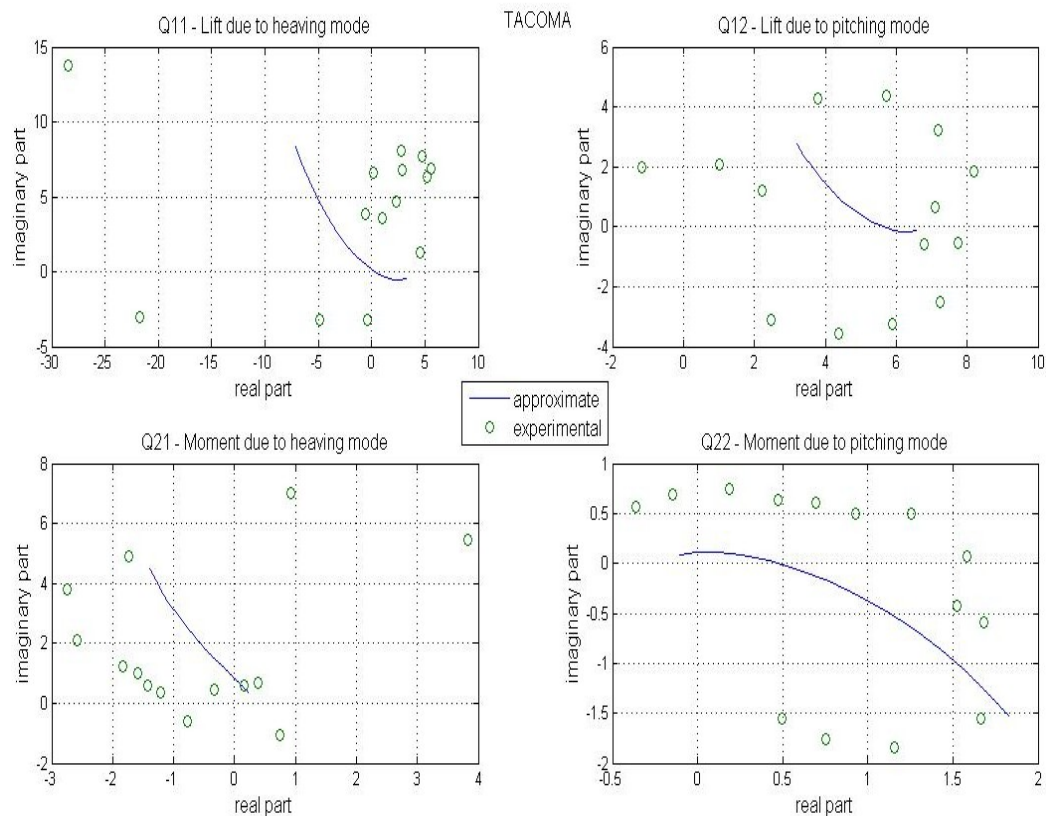


Figure 3-12 - Plots of TC unsteady aerodynamic data

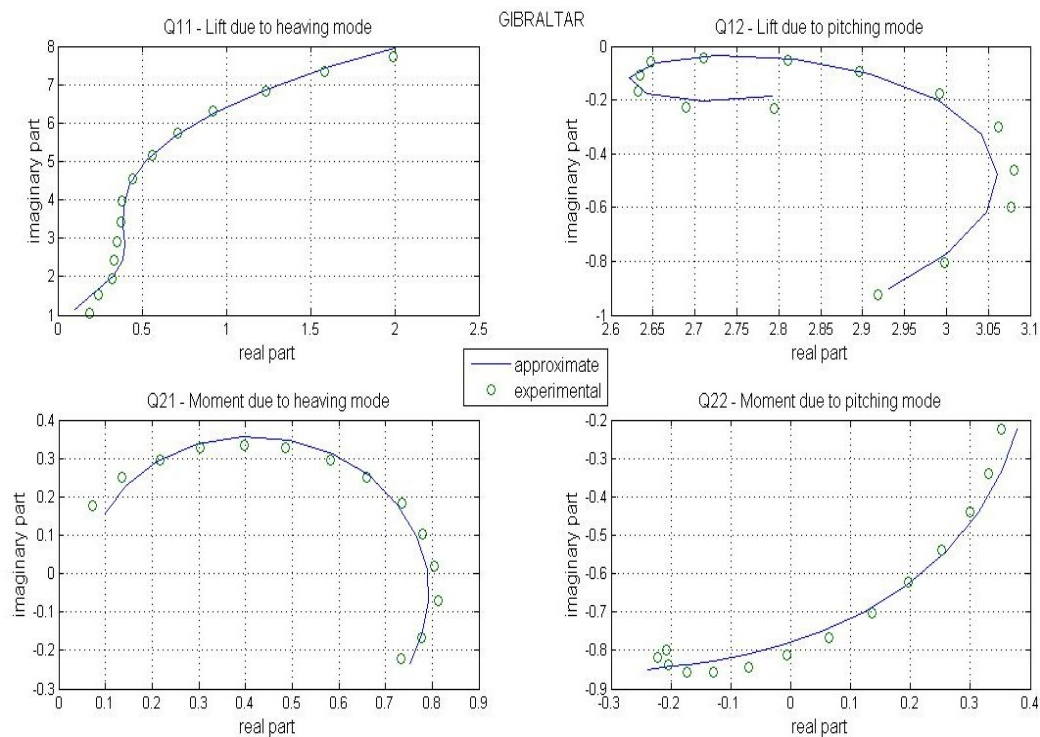


Figure 3-13 - Plots of G unsteady aerodynamic data